Neurobiology of Disease 127 (2019) 350–361

Contents lists available at ScienceDirect

Neurobiology of Disease

journal homepage: www.elsevier.com/locate/ynbdi

Seipin deletion in mice enhances phosphorylation and aggregation of tau protein through reduced neuronal PPARγ and insulin resistance

Huanxian Chang[a,b,1], Tingting Di[a,c,1], Ya Wang[c], Xianying Zeng[d], Guoxi Li[c], Qi Wan[b], Wenfeng Yu[e,**], Ling Chen[a,c,*]

[a] State Key Laboratory of Reproductive Medicine, Nanjing Medical University, Nanjing 211166, China
[b] Department of Neurology, First Affiliated Hospital of Nanjing Medical University, Guangzhou Road 300, Nanjing 210029, China
[c] Department of Physiology, Nanjing Medical University, Nanjing 211166, China
[d] Department of Geratology, First Affiliated Hospital of Nanjing Medical University, Guangzhou Road 300, Nanjing 210029, China
[e] Key Laboratory of Endemic and Ethnic Diseases of Education Ministry, Guizhou Medical University, Guian New District, Guizhou 550025, China

ARTICLE INFO

Keywords:
Seipin
Tau phosphorylation
Peroxisome proliferator-activated receptor-γ (PPARγ)
GSK3β
Mammalian target of rapamycin (mTOR)
Insulin resistance

ABSTRACT

Congenital generalized lipodystrophy 2 (CGL2) is characterized by loss of adipose tissue, insulin resistance and cognitive deficits and caused by mutation of BSCL2/seipin gene. *Seipin* deletion in mice and rats causes severe lipodystrophy, insulin resistance, and cognitive impairment. Hippocampal neurons express seipin protein. This study aimed to investigate the influence of systemic *seipin* knockout (*seipin*-sKO), neuronal *seipin* knockout (*seipin*-nKO) or adipose *seipin* knockout (*seipin*-aKO) in hippocampal tau phosphorylation and aggregation. Levels of tau phosphorylation at Thr^{212}/Ser^{214} and Ser^{202}/Thr^{205} and oligomer tau protein were increased in *seipin*-sKO mice and *seipin*-nKO mice with a decrease in axonal density and expression of PPARγ. Neuronal seipin deletion increased activities of GSK3β and Akt/mTOR signaling, which were corrected by the administration of PPARγ agonist rosiglitazone for 7 days. The autophagosome formation was reduced in *seipin*-sKO mice and *seipin*-nKO mice, which was rescued by the Akt and mTOR inhibitors. The administration of rosiglitazone or Akt, mTOR and GSK3β inhibitors for 7 days could correct the hyperphosphorylation and aggregation of tau. On the other hand, *seipin*-sKO mice appeared insulin resistance and an increase in phosphorylation of tau at Ser^{396} and JNK, which were corrected by treatment with rosiglitazone for 30 days rather than 7 days. Inhibition of JNK in *seipin*-sKO mice corrected the hyperphosphorylated tau at Ser^{396}. The results indicate that neuronal seipin deletion causes hyperphosphorylation and aggregation of tau protein leading to axonal atrophy through reduced PPARγ to enhance GSK3β and Akt/mTOR signaling; systemic seipin deletion-induced insulin resistance causes tau hyperphosphorylation via cascading JNK pathway.

1. Introduction

Congenital generalized lipodystrophy 2 (CGL2) is an autosomal recessive disorder characterized by a near-total loss of adipose tissue, severe insulin resistance and hypertriglyceridemia (Agarwal and Garg, 2003) with intellectual impairment (Rajab et al., 2003; Van Maldergem et al., 2002). The mutation of seipin has been identified in CGL2 patients (Magre et al., 2001; Van Maldergem et al., 2002). *Seipin* knockout in mice and rats causes an early depletion of adipose tissue and insulin resistance (Chen et al., 2012; Prieur et al., 2013), as well as impairments in learning and memory (Ebihara et al., 2015; Zhou et al., 2016). CGL2 patients show a tendency of reduction in whole brain volume

Abbreviations: AD, Alzheimer's disease; BSCL2, Berardinelli-Seip congenital lipodystrophy 2; FPG, fasting plasma glucose; ITT, insulin tolerance test; JNK, c-Jun N-terminal kinase; GSK3β, glycogen synthase kinase-3β; mTOR, mammalian target of rapamycin; NF-H, neurofilament heavy chain; PA, phosphatidic acid; PPARγ, peroxisome proliferator-activated receptor γ; *seipin*-aKO, adipose *seipin* knockout; *seipin*-nKO, neuronal *seipin* knockout; *seipin*-sKO, systemic *seipin* knockout; TOMA, tau oligomer-specific monoclonal antibody

* Correspondence to: L. Chen, State Key Lab of Reproductive Medicine, Department of Physiology, Nanjing Medical University, Tianyuan East Road 818, Nanjing 211166, China.
** Correspondence to: W. Yu, Key Laboratory of Endemic and Ethnic Diseases (Guizhou Medical University), Ministry of Education, Guiyang 550004, Guizhou, China.
E-mail addresses: lingchen@njmu.edu.cn (L. Chen), Wenfengyu2013@126.com (W. Yu).
[1] Contributed equally to this work.

https://doi.org/10.1016/j.nbd.2019.03.023
Received 5 November 2018; Received in revised form 23 February 2019; Accepted 21 March 2019
Available online 22 March 2019
0969-9961/

(Ebihara et al., 2015). Similarly, *seipin* knockout rats appeared an age-related decline in the brain volume.

Cognitive dysfunction is evident in patients with diabetes (Kodl and Seaquist, 2008). Approximately 80% of Alzheimer's disease (AD) patients have diabetes or abnormal blood glucose levels (Janson et al., 2004). Many experimental diabetes animal models also show cognitive dysfunction and AD pathology including hyperphosphorylation of tau (Planel et al., 2007). Rosiglitazone, a peroxisome proliferator-activated receptor-γ (PPARγ) agonist, is effective in improving learning and memory and in ameliorating the hyperphosphorylated tau in AD animal models (Yoon et al., 2010). The administration of rosiglitazone in *seipin* knockout mice not only improves insulin resistance (Prieur et al., 2013), but also rescues cognitive impairment (Denner et al., 2012).

The seipin protein is highly expressed in the hippocampal CA1 pyramidal cells of adult mice (Zhou et al., 2016). Neuronal specific knockout for seipin in mice causes spatial cognitive deterioration (Li et al., 2015). The deletion of seipin is well known to suppress the expression of PPARγ leading to an increase in the activity of GSK-3β (Denner et al., 2012; Planel et al., 2007; Yoon et al., 2010). The mammalian target of rapamycin (mTOR) was activated by the knockout of PPARγ (Sun et al., 2013). The GSK3β or mTOR signaling pathways are involved in the phosphorylation of tau (Zhang et al., 2015). The process of autophagy is negatively regulated by the mTOR signaling. Autophagic dysfunction is thought to cause the hyperphosphorylation of tau and delay the clearance and degradation of tau aggregates (Kruger et al., 2012). Thus, it is of great interest to investigate whether the deficiency of seipin in neuronal cells affects the phosphorylation and aggregation of tau protein leading to neurodegeneration.

In this study, we used 20-week-old male systemic *seipin* knockout (*seipin*-sKO), neuronal *seipin* knockout (*seipin*-nKO) and adipose *seipin* knockout (*seipin*-aKO) mice to investigate the influence of seipin deficiency in hippocampal tau phosphorylation and aggregation. Our results indicate that the neuronal seipin deficiency increased tau phosphorylation at Thr^{212}/Ser^{214} and Ser^{202}/Thr^{205} and tau aggregates with a reduced axonal density; the insulin resistance caused by systemic seipin deficiency increased tau phosphorylation at Ser^{396}. All hyperphosphorylation and aggregation of tau induced by seipin deletion were sensitive to the activation of PPARγ.

2. Materials and methods

2.1. Experimental animals

The procedures involving animals and their care were conducted in conformity with the ARRIVE guidelines of Laboratory Animal Care (Kilkenny et al., 2012). All animal handling procedures followed the guidelines for Laboratory Animal Research of the Nanjing Medical University. The mice were maintained in constant environmental condition (temperature 23 ± 2 °C, humidity 55 ± 5%, and 12:12 h light/dark cycle) and received a standard laboratory diet before and after all procedures. The generation and genotype identification of *seipin*-sKO mice, *nseipin*-nKO mice and *seipin*-aKO mice were performed as described previously (Cui et al., 2011; Liu et al., 2014; Zhou et al., 2016). Twenty-week-old male *seipin*-sKO mice ($n = 30$) and sWT mice ($n = 12$), *seipin*-nKO mice ($n = 36$) and nWT mice ($n = 18$), *seipin*-aKO mice ($n = 12$) and aWT mice ($n = 12$) were randomly divided into 3 experimental groups: the first group was used to measure the fasting plasma glucose and insulin resistance, and subsequently examine the hippocampal structure, the CA1 pyramidal neurons and immunohistochemistry of NF-H; the second group was used to analysis the phosphorylation of tau, PPARγ expression, activities of GSK3β, Akt/mTOR signaling, JNK and p38, and autophagosome formation; the third group was used to explore the molecular mechanisms underlying seipin deficiency-altered tau phosphorylation by combining pharmacological methods. Six hippocampi obtained from 6 mice ($n = 6$) were used in each experimental group.

2.2. Reverse transcription-polymerase chain reaction (RT-PCR)

Real-time PCR was performed as described previously (Zhou et al., 2014). Total RNA was isolated from the hippocampus with TRIzol reagent (Invitrogen, Camarillo, CA) and reverse-transcribed into cDNA using a Prime Script RT reagent kit (Takara, China) for quantitative PCR (ABI Step One Plus, Foster City, CA) in the presence of a fluorescent dye (SYBR Green I; Takara, China). The same sample was examined by two independent RT-PCR analyses. The primers used for seipin (forward 5′-GGCTCCTTCTACTACTCCTACA-3′; reverse 5′-CCGATCACGTCCACT CTT-3′), and GAPDH (forward 5′-ACCACAGTCCATGCCATCAC-3′; reverse 5′-ACCACAGTCCATGCCATCAC-3′) were designed according to the publication (Cui et al., 2011).

2.3. Measurement of plasma glucose and insulin and insulin tolerance test

After mice were fasted for 6 h, the blood was obtained from the tail vein to examine the level of fasting plasma glucose (FPG). The plasma glucose was measured by the glucose oxidase method (Contour Glucometer; Bayer, Toronto, Canada). For the insulin tolerance test (ITT), mice were injected (i.p.) with human recombinant insulin (1 IU/kg, Novolin-R, Novo Nordisk, Plainsboro, NJ, USA) after 6 h of fasting. Blood samples (5 μl/time) were collected from the tail tip at 1 min before insulin injection and at 15, 30, 60, and 120 min after insulin injection as previously described (Hua et al., 2017).

2.4. Antibodies and reagents

The following commercially available antibodies and reagents were used: monoclonal anti-heavychain NF (NF-H) (Santa Cruz sc-137009, Fremont, CA, USA); tau oligomer-specific monoclonal antibody (TOMA) (Millipore, MABN819, Billerica, MA, USA); rabbit anti-PPARγ (Santa Cruz sc-7273); rabbit anti-tau (Abcam ab64193, Cambridge, UK); rabbit anti-tau phosphorylated at Thr^{212}/Ser^{214} (Pierce MN1020, Waltham, Massachusetts, USA), Ser^{202}/Thr^{205} (Pierce MN1060), Ser^{396} (abcam ab109390) or Ser^{235} (abcam ab131354); rabbit anti-GSK3β phosphorylated at Ser^{9} (Cell Signaling Technology 9336S, Inc., Boston, MA, USA) or Tyr^{216} (BD Transduction Laboratories 612313, Lexington, KY, USA); rabbit anti-Akt phosphorylation (Cell Signaling 4060); rabbit anti-mTOR phosphorylation (Cell Signaling 2971); rabbit anti-LC3 (Cell Signaling 4108); rabbit anti-p62 (Cell Signaling 5114); rabbit anti-p38 phosphorylation (Cell Signaling 9212); and anti-JNK phosphorylation (Cell Signaling 9251); mouse anti-β-actin (Abbkine A01010, Redlands, CA, USA); anti-Akt (Cell Signaling 9272); rabbit anti-mTOR (Cell Signaling 2972); rabbit anti-GSK3β (Cell Signaling Technology 9315); anti-p38 (rabbit; Cell Signaling 8690); anti-JNK (Cell Signaling 9252); anti-β-actin (Abbkine A01010, Redlands, CA, USA); Rosiglitazone (Enzo, Farmingdale, NY); AR-A014418, rapamycin, LY294002; SP600125 (Sigma-Aldrich, St. Louis, MO, USA).

2.5. Histological examination of hippocampus

Mice were anesthetized with pentobarbital (50 mg/kg, i.p.) and perfused transcardially with 4% paraformaldehyde. Brains were removed and processed for paraffin embedding. Coronal sections (5 μm) were placed on gelatin-coated slides. Toluidine blue staining was performed using standard protocols. Images of stained sections were acquired on a conventional light microscope (Olympus DP70, × 40, Tokyo, Japan). The density of CA1 pyramidal cells was expressed as the number of cells per mm length measured along the cell layer (Cai et al., 2008).

For immunohistochemistry of NF-H, the sections were blocked with 3% normal goat serum, and then incubated with the primary first antibody, monoclonal anti-heavychain NF (NF-H) (1:1000) at 4 °C

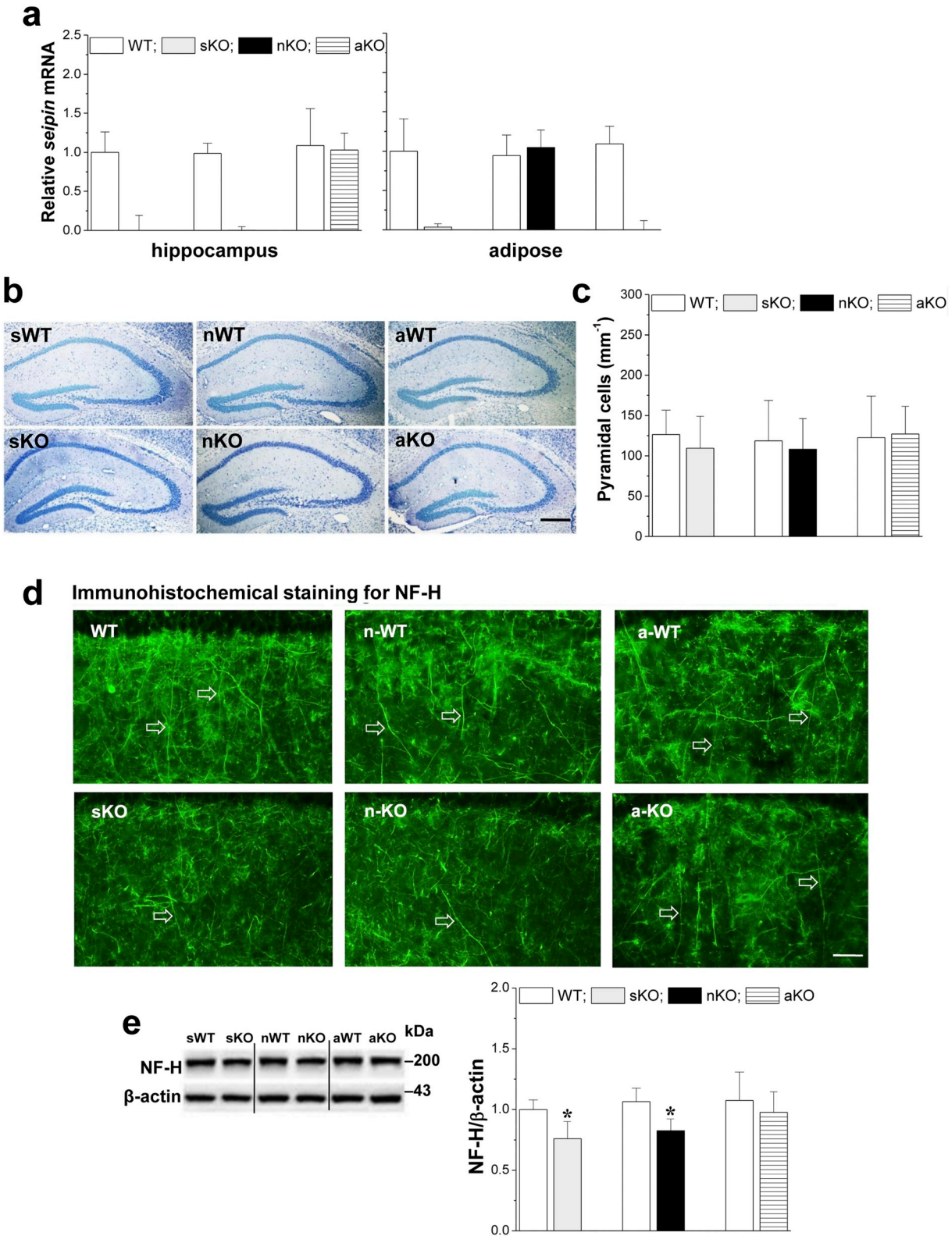

Fig. 1. Neuronal seipin deficiency caused axonal degeneration. (a) Detection of seipin expression is examined by quantitative real-time PCR in hippocampus and adipose tissues of *seipin*-sKO mice and sWT mice, *seipin*-nKO mice and nWT mice, *seipin*-aKO mice and aWT mice. (b) Representative images of the hippocampal CA1 regions (5 μm sections stained with toluidine blue). Scale bars = 20 μm. (c) Bars represent the density of pyramidal cells in CA1 and CA3 regions. (d) Representative photomicrographs of immunohistochemical staining for neurofilament heavy chain (NF-H) to visualize NF proteins in the hippocampal CA1 radium layer. White arrows indicate NF-H positive fibers. Scale bars = 200 μm. (e) Levels of NF-H protein in hippocampus. *$P < .05$ vs. n/sWT mice (Student's *t*-test).

overnight. Immunoreactivities were detected by an Alexa Fluor 488 conjugated secondary antibody (1:200, Jackson ImmunoResearch Laboratories, PA, USA) using a fluorescence microscope (Olympus DP70) with ×40 objective.

2.6. Western blot analyses

Hippocampus were homogenized in 200 μl Tris buffer (10% sucrose and protease inhibitors, pH 7.4, Complete; Roche Diagnostics) and sonicated. The homogenates were centrifuged for 15 min (Thermo Scientific) and the supernatants were collected. Proteins (20–40 μg) were loaded for separation by SDS-PAGE and transferred to nitrocellulose membranes. Membranes were incubated with blocking solution (5% nonfat dried milk) for 1 h at room temperature, and then incubated with primary antibodies of anti-NF-H (1:1000), anti-PPARγ (1:1000); anti-tau (1:2000); anti-phosphorylation of tau at Thr^{212}/Ser^{214}, Ser^{202}/Thr^{205}, Ser^{396} or Ser^{235} (1:1000); anti-phosphorylation of GSK3β at Ser^{9} or Tyr^{216} (1:1000); anti-phosphorylation of Akt and mTOR (1:1000); anti-LC3 and anti-p62 (1:1000); anti-phosphorylation of p38 and JNK (1:2000); TOMA (1:250) at 4 °C overnight. After washes with TBST, the membranes were incubated for 1 h with HRP-labeled secondary antibodies, and developed using the ECL detection kit (Amersham Biosciences). Following visualization, the blots were stripped by incubation in stripping buffer (Restore; Pierce Biotechnology, Inc., Rockford, IL, USA) for 15 min and then incubated with antibodies of β-actin, Akt, mTOR, GSK3β, p38 and JNK (1:1000). There were two independent experiments were performed for each sample. Western blot bands were scanned and analyzed with the image analysis software package (Image J; NIH Image, Bethesda, MD, USA).

2.7. Administration of drugs

Rosiglitazone, AR-A014418, rapamycin, LY294002 and SP600125 were dissolved in dimethyl sulfoxide (DMSO) and then diluted in 0.9% saline to a final concentration of 0.5% DMSO. Oral administration of rosiglitazone (4 mg/kg) (Wring et al., 2018); intraperitoneal injection (i.p.) of AR-A014418 (1 mg/kg) (Martins et al., 2011); rapamycin (1 μg/kg) (Li et al., 2010); SP600125 (10 mg/kg) (Hu et al., 2016) were given daily. For repeated injection (i.c.v.) of drug, mice were anesthetized with ketamine (100 mg/kg, i.p.) and xylazine (10 mg/kg, i.p.), then placed in a stereotactic apparatus (Motorized Stereotaxic StereoDrive; Neurostar). A small hole (2 mm diameter) was drilled in the skull using a dental drill, and a 26-G stainless steel guide cannula (Plastics One, Roanoke, VA, USA) was implanted into the right lateral ventricle (0.3 mm posterior to bregma, 1.0 mm lateral, and 2.3 mm ventral) and anchored to the skull with 3 stainless steel screws and dental cement. The injection (i.c.v.) of LY294002 (0.3 nmol/3 μl/mouse) (Owen et al., 2014) was given using a stepper-motorized micosyringe (Stoelting, Wood Dale, IL, USA). The mice injected (i.c.v.) with vehicle (0.1% DMSO) at same volume were served as the control group.

2.8. Data analysis/statistics

All experimental results were retrieved and processed with Micro cal Origin 9.1. All data were presented as the means ± standard difference (S.D.). Data were statistically examined using SPSS software (version 18.0, SPSS, USA). Two-group analysis was performed by Student's *t*-test (normally distributed data) or the Mann-Whitney-test (non-normally distributed data). For multiple comparison groups, analyses of variance (ANOVA) with the Bonferroni post hoc test were performed under homogeneity of variance. Repeated-measures ANOVA was used for the insulin tolerance test. Differences at $P < .05$ were considered statistically significant.

3. Results

3.1. Neuronal seipin deletion reduces axonal density in hippocampus

The seipin is highly expressed in hippocampal pyramidal cells of rats and mice (Ebihara et al., 2015; Magre et al., 2001; Zhou et al., 2016). To investigate the effects of the seipin deficiency on the hippocampal tau phosphorylation, we in this study used 20-week-old systemic seipin knockout (*seipin*-sKO) mice, neuronal seipin knockout (*seipin*-nKO) mice and adipose seipin knockout (*seipin*-aKO) mice. The analysis of RT-PCR showed the selective deletion of seipin expression in the hippocampus of *seipin*-nKO mice and the adipose of *seipin*-aKO mice (Fig. 1a). The hippocampal size and morphological structure of the CA1 and CA3 regions or dentate gyrus in *seipin*-sKO mice, *seipin*-nKO mice or *seipin*-aKO mice did not differ greatly from those of age-matched sWT mice, nWT mice and aWT-mice ($n = 6$ mice per experimental group; Fig. 1b). Although *seipin*-aKO mice and *seipin*-nKO mice had a tendency to decrease the density of CA1 pyramidal cells, the group when compared with aWT mice and nWT mice failed to reach the significance ($P > .05$, $n = 6$; Fig. 1c).

The immunohistochemical staining for neurofilament heavy chain (NF-H) showed that the density of NF-H positive fibers in the CA1 radium layer was obviously diminished in *seipin*-sKO mice and *seipin*-nKO mice compared to that of WT mice (Fig. 1d). The NF-H positive fibers seem to be shorter and thinner in *seipin*-sKO mice or *seipin*-nKO mice. Additionally, the levels of hippocampal NF-H protein obtained from *seipin*-sKO mice ($P < .05$, $n = 6$; Fig. 1e) or *seipin*-nKO mice ($P < .05$, $n = 6$) were lower than those of WT mice. By contrast, the density of NF-H positive fibers or the levels of NF-H protein showed no significant differences between *seipin*-aKO mice and aWT-mice ($P > .05$, $n = 6$; Fig. 1e). The results indicated that neuronal seipin deletion causes loss of hippocampal axon.

3.2. Neuronal seipin deletion increased hippocampal tau phosphorylation

Tau, a microtubule-associated protein, dynamically regulates the polymerization, stability, and assembly of axonal microtubules (Gendron and Petrucelli, 2009). In comparison with corresponding controls, the levels of tau protein in hippocampus of *seipin*-sKO mice, *seipin*-nKO mice and *seipin*-aKO mice failed to be altered ($P > .05$, $n = 6$ mice per experimental group; Fig. 2a). Subsequently, we examined the higher molecular weight tau protein using a tau oligomer-specific monoclonal antibody (TOMA) (Leyk et al., 2015). As shown in Fig. 2b, the levels of oligomeric tau in *seipin*-sKO mice ($P < .05$, $n = 6$) and *seipin*-nKO mice ($P < .05$, $n = 6$) were higher than those in WT mice.

Tau hyperphosphorylation is site specific and mainly occurs at serine/threonine residues, such as Thr^{212}, Thr^{205}, Ser^{396}, Ser^{214}, Ser^{262}, and Ser^{202} (Wang et al., 2014), because serine/threonine protein kinases and phosphatases regulate tau phosphorylation directly. Using analyses of western-blot, we examined the levels of tau phosphorylated (phospho-tau) at Thr^{212}/Ser^{214} (AT100 site), Ser^{202}/Thr^{205} (AT8 site), Ser^{396} (PHF-1 site) and Ser^{235} (TG3 site) ($n = 6$ mice per experimental group). Notably, *seipin*-sKO mice showed an approximately 1.6-fold increase in the levels of phospho-tau at Thr^{212}/Ser^{214} ($P < .01$; Fig. 2c) and Ser^{202}/Thr^{205} ($P < .05$) with a 1.3-fold elevation of phospho-tau at Ser^{396} ($P < .05$) compared to sWT mice, while Ser^{235} had no significant difference compared to sWT mice ($P > .05$). By contrast, the levels of phospho-tau at Thr^{212}/Ser^{214} ($P < .01$) and Ser^{202}/Thr^{205} ($P < .01$) in *seipin*-nKO mice were increased by nearly 1.7-fold compared with those in nWT mice, but at Ser^{396} ($P > .05$) or Ser^{235} ($P > .05$) no difference was observed. Only the phospho-tau at Ser^{396} had a tendency to increase in *seipin*-aKO mice ($P > .05$). The results show that neuronal seipin deletion enhances tau phosphorylation at Thr^{212}/Ser^{214} and Ser^{202}/Thr^{205}.

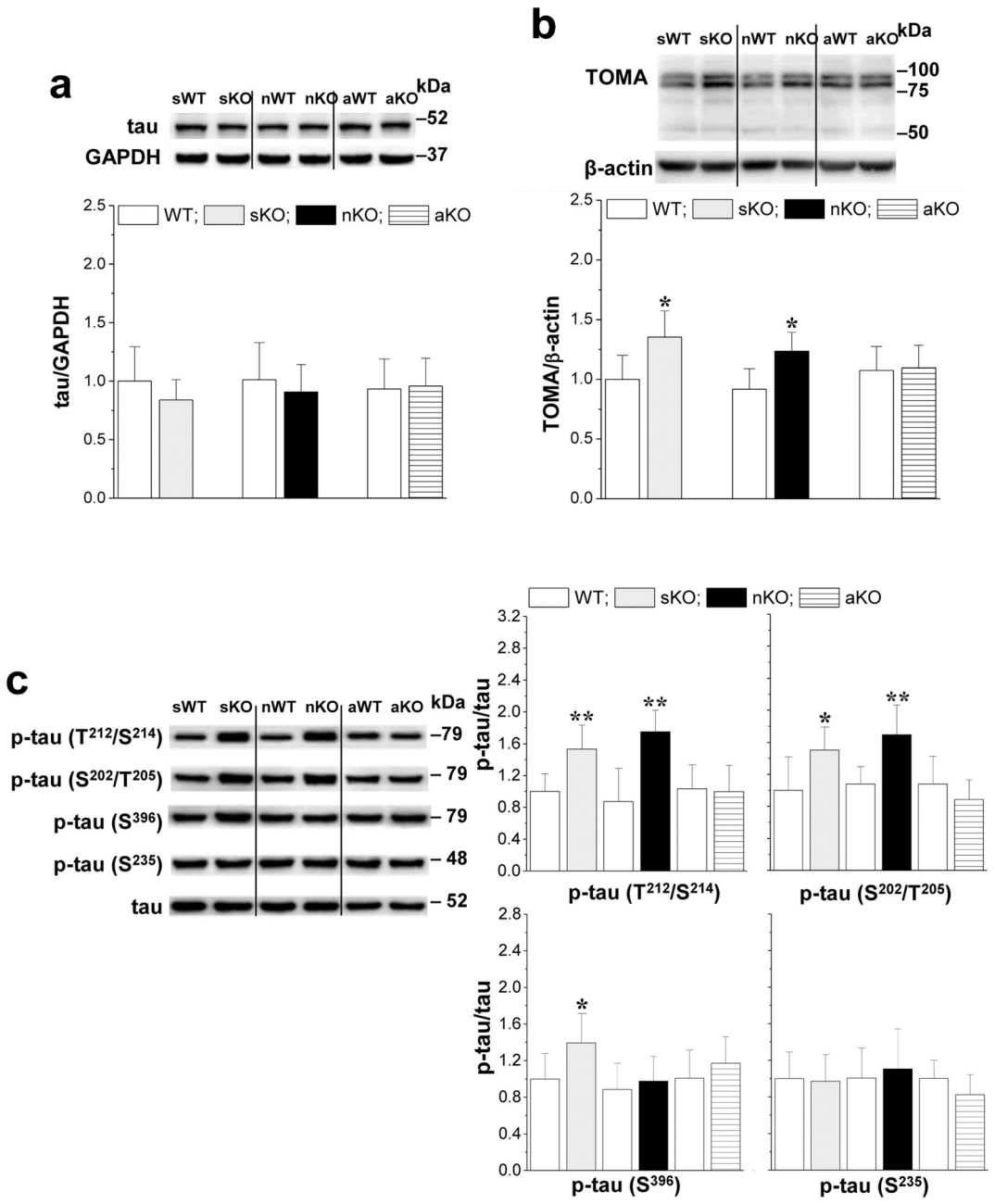

Fig. 2. Neuronal seipin deficiency increased hippocampal tau phosphorylation. (a and b) Levels of monomeric tau and oligomer tau protein in hippocampus from *seipin*-sKO mice, *seipin*-nKO mice, *seipin*-aKO mice and WT mice. $^{*}P < .05$ vs. s/nWT mice (Student's *t*-test). (c) Levels of tau phosphorylation (p-tau) at Thr^{212}/Ser^{214}, $Ser^{202}/^{205}$, Ser^{396} and ser^{235} epitopes. $^{*}P < .05$ and $^{**}P < .01$ vs. s/nWT mice (Student's *t*-test).

3.3. Seipin deletion by reducing PPARγ increased tau phosphorylation

The decline in hippocampal PPARγ protein in *seipin*-sKO mice and *seipin*-nKO mice is thought to lead to cognitive deterioration (Zhou et al., 2016). Further experiments were designed to examine the involvement of reduced PPARγ in tau hyperphosphorylation at Thr^{212}/Ser^{214}, Ser^{202}/Thr^{205} and ser^{396} ($n = 6$ mice per experimental group). The levels of hippocampal PPARγ protein were significantly reduced in *seipin*-sKO mice ($P < .01$; Fig. 3a) or *seipin*-nKO mice ($P < .01$) rather than *seipin*-aKO mice ($P > .05$) compared to those of WT mice. Treatment with rosiglitazone (rosi, 4 mg/kg) for 7 days in *seipin*-sKO mice remarkably corrected the increase in the levels of phospho-tau at Thr^{212}/Ser^{214} ($P < .05$; Fig. 3b) and Ser^{202}/Thr^{205} ($P < .05$), but had no effect on the level of phospho-tau at ser^{396} ($P > .05$). The results indicate that the seipin deletion through reduced PPARγ enhances tau phosphorylation at Thr^{212}/Ser^{214} and Ser^{202}/Thr^{205}.

3.4. Involvement of seipin deletion-elevated GSK3β activity in tau phosphorylation

Seipin deficiency has been found to increase the GSK3β activity by reducing PPARγ (Qian et al., 2016). To investigate whether GSK3β activity is involved in the tau hyperphosphorylation of *seipin*-nKO mice, we examined the hippocampal phosphorylation of GSK3β (phospho-GSK3β) at Tyr^{216} and Ser^{9}, respectively ($n = 6$ mice per experimental group). In comparison with WT mice, the level of phospho-GSK3β at Tyr^{216} were increased in *seipin*-sKO mice ($P < .05$; Fig. 4a) or *seipin*-nKO mice ($P < .05$; Fig. 4a), while the level of phospho-GSK3β at Ser^{9} was decreased (sKO: $P < .01$; nKO: $P < .05$), which could be corrected by the administration of rosi (4 mg/kg) for 7 days (sKO-Tyr^{216}:

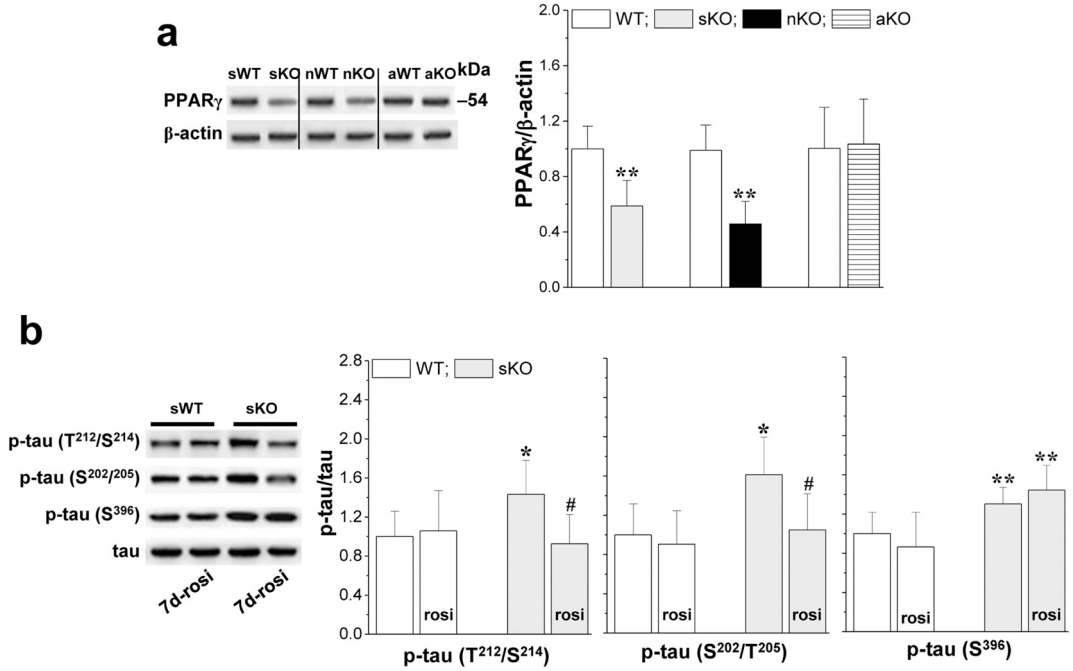

Fig. 3. Seipin deficiency through reducing PPARγ increased tau phosphorylation. (a) Levels of hippocampal PPARγ protein in the *seipin*-sKO mice, *seipin*-nKO mice, *seipin*-aKO mice and WT mice. $^{**}P < .01$ vs. n/sWT mice (Student's *t*-test). (b) Bar graph shows the levels of tau phosphorylation (p-tau) at Thr^{212}/Ser^{214}, Ser^{202}/Thr^{205} and Ser^{396} in the *seipin*-sKO mice and sWT mice treated with rosiglitazone (rosi) for 7 days. $^{*}P < .05$ and $^{**}P < .01$ vs. sWT mice; $^{\#}P < .05$ and $^{\#\#}P < .01$ vs. *seipin*-sKO mice (two-way ANOVA).

$P < .01$; nKO-Tyr^{216}: $P < .05$; sKO-$pSer^{9}$: $P < .01$; nKO-$pSer^{9}$: $P < .05$). Furthermore, the treatment with the GSK3β inhibitor AR-A014418 (AR, i.c.v.) for 7 days in *seipin*-nKO mice could prevent the increase in the phospho-tau at Thr^{212}/Ser^{214} ($P < .05$; Fig. 4b) and Ser^{202}/Thr^{205} ($P < .05$), although it did not alter the level of phospho-tau at Thr^{212}/Ser^{214} ($P > .05$) and Ser^{202}/Thr^{205} ($P > .05$) in nWT mice. The results indicate that the seipin deletion through reduced PPARγ elevates the GSK3β activity, which enhances tau phosphorylation at Thr^{212}/Ser^{214} and Ser^{202}/Thr^{205}.

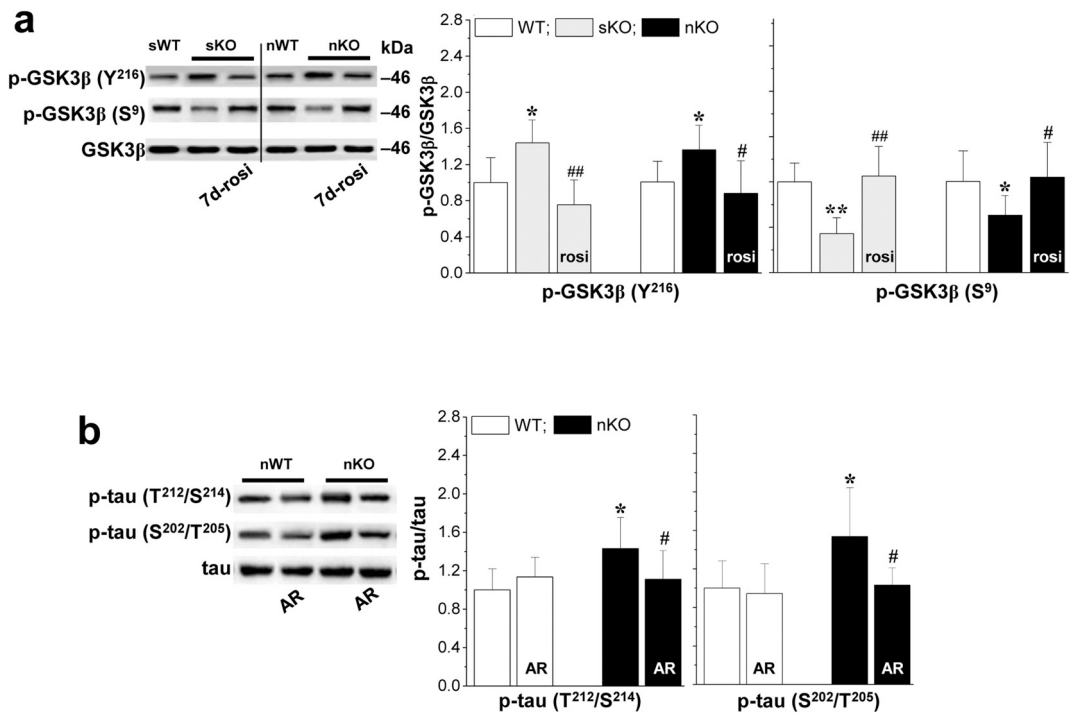

Fig. 4. Seipin deficiency elevated GSK3β activities by reducing PPARγ. (a) Bars represent levels of GSK3β phosphorylation (p-GSK3β) at Tyr^{216} (left panel) and Ser^{9} (right panel) in the *seipin*-sKO mice, *seipin*-nKO mice and WT mice treated with rosiglitazone (rosi). $^{*}P < .05$ and $^{**}P < .01$ vs. s/nWT mice; $^{\#}P < .05$ and $^{\#\#}P < .01$ vs. *seipin*-s/nKO mice (one-way ANOVA). (b) Bar graphs show the tau phosphorylation (p-tau) at Thr^{212}/Ser^{214} and Ser^{202}/Thr^{205} in *seipin*-nKO mice and nWT mice treated with AR-A014418 (AR). $^{*}P < .05$ and $^{**}P < .01$ vs. nWT mice; $^{\#}P < .05$ and $^{\#\#}P < .01$ vs. *seipin*-nKO mice (two-way ANOVA).

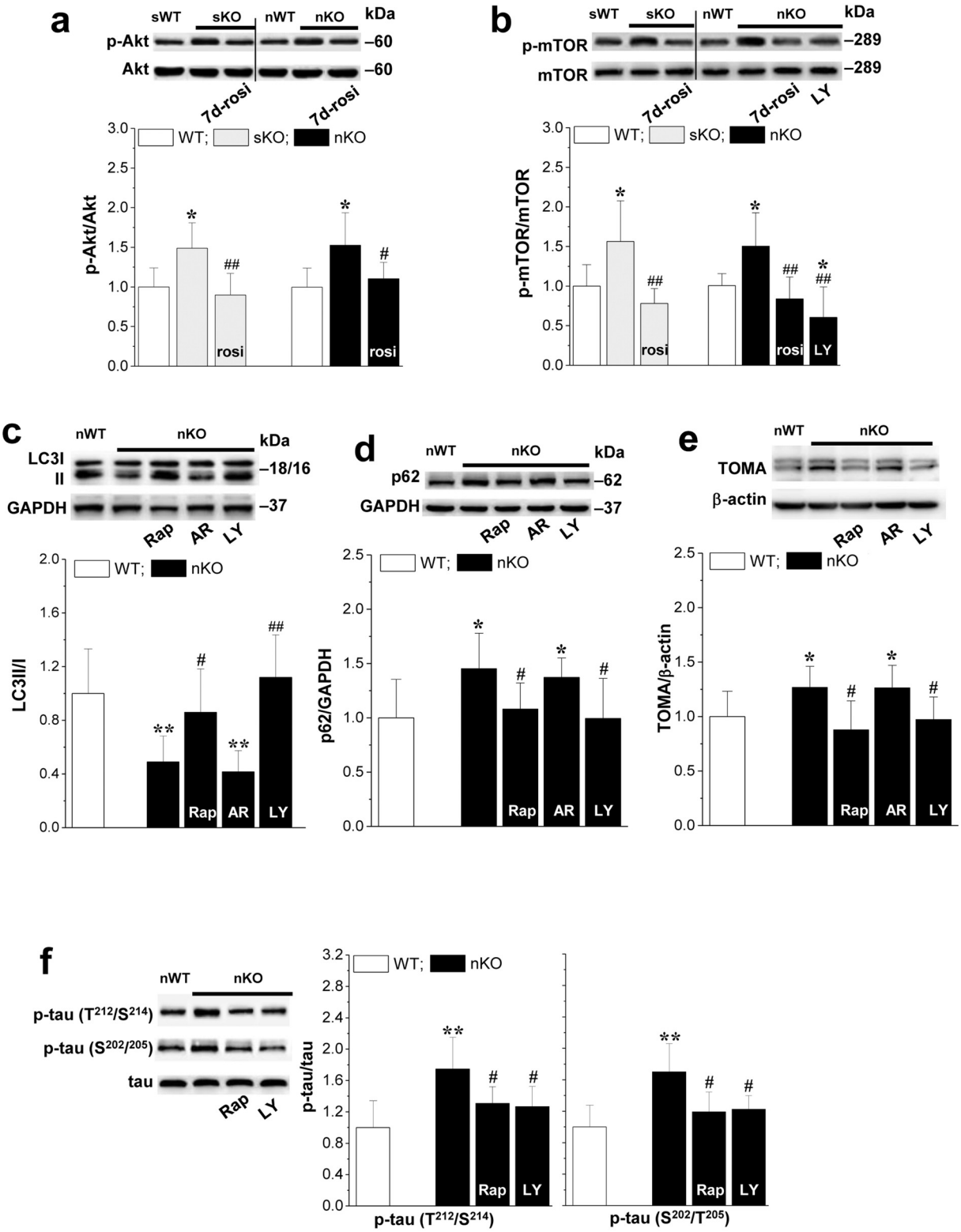

Fig. 5. Seipin deficiency increased Akt-mTOR signaling to suppress autophagy. (a and b) Levels of phosphorylated Akt (p-Akt) and mTOR (p-mTOR) in *seipin*-sKO mice, *seipin*-nKO mice and WT mice treated with rosiglitazone (rosi) or LY294002 (LY). $^{*}P < .05$ and $^{**}P < .01$ vs. s/nWT mice; $^{\#}P < .05$ and $^{\#\#}P < .01$ vs. *seipin*-s/nKO mice (one-way ANOVA). (c and d) Bar graphs show the ratio of LC3-II/LC3-I and the level of p62 in the hippocampus of *seipin*-nKO mice treated with rapamycin (Rap), LY294002 (LY) and AR-A014418 (AR). $^{*}P < .05$ and $^{**}P < .01$ vs. nWT mice; $^{\#}P < .05$ and $^{\#\#}P < .01$ vs. *seipin*-nKO mice (one-way ANOVA). (e and f) Levels of oligomer tau protein and tau phosphorylation (p-tau) at Thr^{212}/Ser^{214} and Ser^{202}/Thr^{205} in *seipin*-nKO mice treated with rapamycin (Rap) and LY294002 (LY). $^{**}P < .01$ vs. nWT mice; $^{\#}P < .05$ vs. *seipin*-nKO mice (one-way ANOVA).

3.5. Effects of seipin deletion-enhanced Akt-mTOR signaling on tau phosphorylation

The activation of PPARγ by its ligands induces autophagy (Zhou et al., 2009). The mTOR signaling is well known to be a major negative regulator of autophagy (Zhang et al., 2015). To test whether the seipin deletion through reduced PPARγ affects the autophagy, we examined the phosphorylation of hippocampal Akt (phospho-Akt) and mTOR (phospho-mTOR), the levels of the autophagy-related proteins LC3 and p62 ($n = 6$ mice per experimental group). The levels of phospho-Akt ($P < .05$; Fig. 5a) and phospho-mTOR ($P < .05$; Fig. 5b) were increased in *seipin*-sKO mice or *seipin*-nKO mice compared with those in WT mice. The increased phospho-Akt (sKO: $P < .01$; nKO: $P < .05$) and phospho-mTOR ($P < .01$) in *seipin*-sKO mice or *seipin*-nKO mice were normalized by the administration of rosi (4 mg/kg) for 7 days. The increased phospho-mTOR in *seipin*-nKO mice was sensitive to the administration of PI3K inhibitor LY294002 (LY, i.c.v.) for 7 days ($P < .01$).

LC3-I is post-translationally modified during autophagy induction to form LC3-II, thus LC3II/I is an index of autophagosome formation (Leyk et al., 2015). As shown in Fig. 5c, the level of LC3-I in *seipin*-nKO mice did not differ significantly from that in WT mice, but the LC3-II level was decreased, leading to a decrease in the ratio of LC3II/I ($P < .01$). In addition, *seipin*-nKO mice had a more intense p62 band ($P < .05$; Fig. 5d), an autophagic substrate. Notably, the reduction in LC3II/I and the elevation of p62 in *seipin*-nKO mice could be corrected by the treatment with the mTOR inhibitor rapamycin (Rap, $P < .05$) or LY294002 (LC3II/I: $P < .01$; p62: $P < .05$) for 7 days, but not AR-A014418 ($P > .05$). The treatment of *seipin*-nKO mice with either rapamycin or LY294002 for 7 days could reduce the levels of oligomeric tau protein ($P < .05$; Fig. 5e) and the phospho-tau at Thr^{212}/Ser^{214} ($P < .05$; Fig. 5f) and Ser^{202}/Thr^{205} ($P < .05$), but not the level of monomeric tau. The results indicate that the reduced PPARγ by seipin deletion suppresses the autophagosome formation through the enhanced Akt-mTOR signaling, leading to an increase in the phosphorylation and aggregation of tau protein.

3.6. Influence of seipin deletion-induced insulin resistance in tau phosphorylation

The levels of fasting plasma glucose showed no significant difference between the *seipin*-sKO mice, *seipin*-nKO mice or *seipin*-aKO and WT mice ($P > .05$, $n = 6$; Fig. 6a). In the insulin tolerance test (ITT), the plasma glucose levels at 15 min, 30 min and 60 min after the injection of insulin in *seipin*-sKO mice were higher than those in sWT mice (15 min: $P < .01$; 30 min, 60 min: $P < .05$, $n = 6$; Fig. 5b), which could be partially corrected by the administration of rosi (4 mg/kg) for 30 days. The *seipin*-aKO mice showed a tendency to decrease the insulin sensitivity, but, the group when compared with aWT mice failed to reach the significance ($P > .05$, $n = 6$). The results of ITT did not show the insulin resistance in *seipin*-nKO mice ($P > .05$, $n = 6$).

Because the phospho-tau at Ser^{396} was increased in *seipin*-sKO mice rather than *seipin*-nKO mice or *seipin*-aKO mice, further experiments were designed to explore the effects of abnormal glucose metabolism on the phospho-tau at Ser^{396} ($n = 6$ per experimental group). Notably, the hippocampal phosphorylation of c-Jun N-terminal kinase (JNK) (phospho-JNK) in *seipin*-sKO mice was increased compared to that in sWT mice ($P < .01$; Fig. 6c), which was corrected by 30 days treatment with rosi ($P < .01$), but not the 7 days treatment ($P > .05$), or the administration of AR-A014418 ($P > .05$) and rapamycin ($P > .05$). The *seipin*-nKO mice did not show the change in the phospho-JNK ($P > .05$). In addition, the levels of P38 phosphorylation (phospho-P38) in *seipin*-sKO mice or *seipin*-nKO mice did not differ from those of WT mice ($P > .05$; Fig. 6d). Moreover, treatment with the JNK inhibitor SP600125 (SP, i.c.v.) for 7 days in *seipin*-sKO mice could recover the level of phospho-tau at Ser^{396} ($P < .05$; Fig. 6e), whereas it had no effects on the elevation of Thr^{212}/Ser^{214} ($P > .05$) and Ser^{202}/Thr^{205} ($P > .05$). The increased phospho-tau at Ser^{396} was corrected by 30 days treatment with rosi ($P < .05$). The results indicate that the seipin deletion causes insulin resistance cascading JNK pathway to induce hyperphosphorylated tau at Ser^{396}.

4. Discussion

In the present study, we used the *seipin*-sKO mice, *seipin*-nKO mice and *seipin*-aKO mice and provided in vivo evidence that the neuronal seipin deletion through reducing PPARγ increased tau phosphorylation at Thr^{212}/Ser^{214} and Ser^{202}/Thr^{205} and the level of soluble oligomeric tau; the systemic seipin deletion caused insulin resistance leading to increase in tau phosphorylation at Ser^{396}. The increased phosphorylation of tau leads to axon transport deficits and mitochondrial dysfunction, resulting in axonal atrophy (Mocanu et al., 2008; Watari and Shimada, 2014). Indeed, the density of NF-H positive neurites and the level of NF-H protein in *seipin*-sKO mice or *seipin*-nKO mice were decreased, indicating the axonal atrophy or loss.

Consistent with a recent report by Qian et al. (2016), the catalytic activity of GSK3β was increased in hippocampus of *seipin*-sKO mice and *seipin*-nKO mice, as showed by the increased phospho-GSK3β at Tyr^{216} and the reduced phospho-GSK3β at Ser^{9}. Similarly, the GSK3β activity in substantia nigra pars compacta (SNpc) of *seipin*-nKO mice was higher than that in nWT mice (Wang et al., 2018). The phosphatidylinositol 3-kinase (PI3K)/Akt signaling can induce the activation of GSK3β, which is abrogated by the PPARγ antagonist GW9662 (Zhang et al., 2018). In particular, the increased GSK3β activity by seipin deficiency was sensitive to the PPARγ agonist or inhibition of PI3K, but not the inhibition of mTOR (data not shown). The PPARγ agonists have been described to be non-ATP competitive GSK3β inhibitors (Inestrosa et al., 2005; Martinez et al., 2002). GSK3β is thought to be a positive mediator of tau phosphorylation, since elevated GSK3β activity correlates with tau hyperphosphorylation at the Ser^{202}/Thr^{205}; inhibited GSK3β activity reduces tau phosphorylation (Plattner et al., 2006). GSK3 generates phospho-epitopes on tau (Nishimura et al., 2004) and co-localizes with aggregates of hyperphosphorylated tau (Ishizawa et al., 2003). The GSK3β inhibitor could also correct the hyperphosphorylated tau at Thr^{212}/Ser^{214} and Ser^{202}/Thr^{205} in *seipin*-nKO mice. Thus, it is conceivable that the neuronal seipin deletion through reduced PPARγ enhances GSK3β activity, which is involved in the hyperphosphorylation of tau (Fig. 7).

A critical finding in this study is that the levels of hippocampal Akt or mTOR phosphorylation were significantly elevated in *seipin*-sKO mice and *seipin*-nKO mice, which were recovered by the activation of PPARγ. The Akt/mTOR signaling pathway was activated by the knockout of PPARγ or the PPARγ antagonist (Sun et al., 2013). The increased mTOR phosphorylation in the *seipin*-nKO mice was abolished by the PI3K inhibitor, indicating that the high activation of Akt directly phosphorylates mTOR (Harrington et al., 2005). Furthermore, the PPARγ deficiency is reported to increase the expression of mTOR (Vasheghani et al., 2015). However, *seipin*-sKO mice and *seipin*-nKO mice did not show the changes in the expression level of mTOR. Importantly, the Akt or mTOR inhibitor could prevent the hyperphosphorylation of tau at Thr^{212}/Ser^{214} and Ser^{202}/Thr^{205} in *seipin*-nKO mice. The contribution of mTOR signaling on tau phosphorylation and degradation has been confirmed by numerous studies, in which increasing mTOR activity can elevate endogenous tau phosphorylation in mice; pharmacologically reducing mTOR activity ameliorates the tau phosphorylation and tau pathology in a mouse model over-expressing mutant human tau (Caccamo et al., 2013); and tau phosphorylation is significantly reduced in 3xTg-AD mice treated with rapamycin (Caccamo et al., 2010).

It has been reported that rapamycin can decrease tau phosphorylation at Ser^{214} via the regulation of cAMP-dependent kinase, leading to less build-up of hyperphosphorylated tau (Liu et al., 2013). The

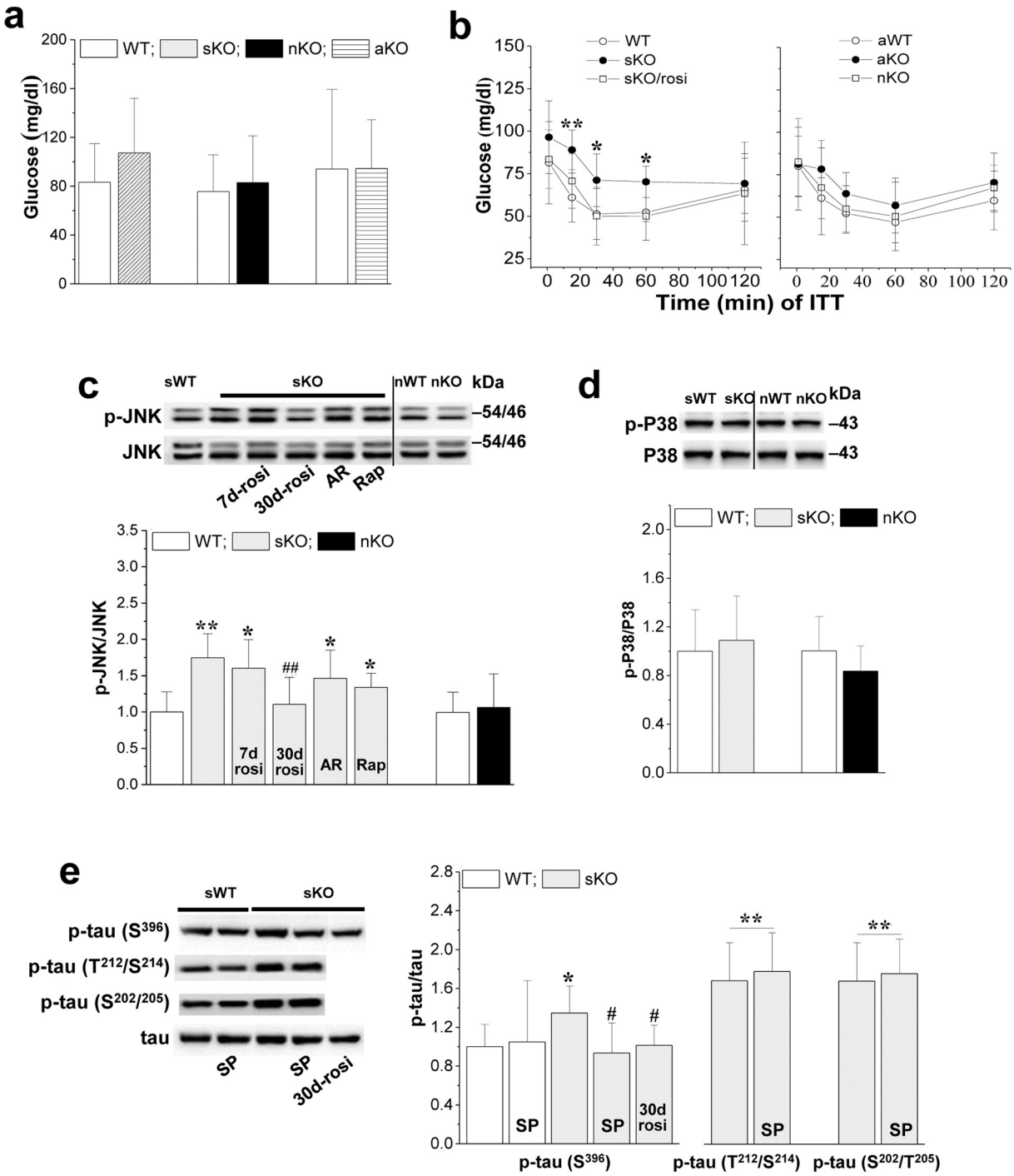

Fig. 6. Seipin deletion-induced insulin resistance enhanced tau phosphorylation. (a and b) Fasting serum insulin (FSI) and levels of plasma glucose during insulin tolerance tests (ITT) in the *seipin*-sKO mice, *seipin*-nKO mice, *seipin*-aKO mice and WT mice. $^{*}P < .05$ and $^{**}P < .01$ vs. sWT mice; $^{\#}P < .05$ and $^{\#\#}P < .01$ vs. *seipin*-sKO mice (one-way ANOVA). (c and d) Bar graphs show the levels of JNK (p-JNK) and P38 (p-P38) phosphorylation in the *seipin*-sKO mice, *seipin*-nKO mice, WT mice and *seipin*-sKO mice treated with rosiglitazone (rosi), AR-A014418 (AR) and rapamycin (Rep). $^{**}P < .01$ vs. sWT mice; $^{\#\#}P < .01$ vs. *seipin*-sKO mice (one-way ANOVA). (e) Bar graph shows the tau phosphorylation (p-tau) at Ser^{396}, Thr^{212}/Ser^{214} and Ser^{202}/Thr^{205} in the *seipin*-sKO mice treated with SP600125. $^{**}P < .01$ vs. sWT mice; $^{\#}P < .05$ vs. *seipin*-sKO mice (one-way ANOVA).

activation of PPARγ in APP transgenic mice reduced tau pathology (Escribano et al., 2010), probably through enhanced brain clearance (Camacho et al., 2004). Autophagy is a cellular homeostatic process involving the turnover of organelles and proteins by the lysosome-dependent degradation pathway (Levine and Kroemer, 2008; Mizushima et al., 2008). PPARγ is involved in the regulation of the mTOR-autophagy pathway (Vasheghani et al., 2015). The activation of autophagy has been demonstrated to reduce the tau aggregation, since the tau aggregates are degraded via the autophagic pathway (Ji et al., 2019). The initiation of autophagy can enhance tau clearance in vivo and in vitro (Zhang et al., 2017). The autophagic dysfunction might reduce the degradation of tau aggregates leading to the deposition of tau proteins (Schaeffer and Goedert, 2012). The enhanced autophagy by the mTOR inhibitor can increase the clearance of hyperphosphorylated tau (Cai et al., 2012). In the hippocampus of *seipin*-sKO mice and *seipin*-nKO mice, the ransformation of LC3I to LC3II was reduced with an increase

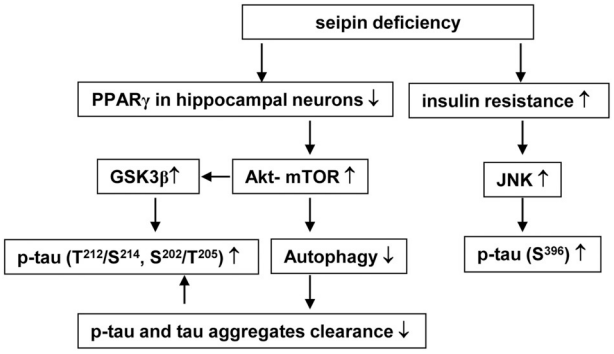

Fig. 7. The hypothesis of molecular mechanisms underlying the seipin deficiency-enhanced tau phosphorylation. ↑: increase; ↓: decrease.

in p62 level, indicating a deficit in the autophagosome formation. The autophagosome formation in *seipin*-nKO mice was recovered by the activation of PPARγ and the inhibition of PI3K or mTOR. Thus, it is proposed that the seipin deletion through reduced PPARγ increases mTOR activity, which suppresses autophagy to reduce the autophagic clearance of tau protein and to enhance the tau aggregation (Fig. 7). The idea is supported by the experimental results that the level of soluble oligomeric tau protein was increased in *seipin*-sKO mice and *seipin*-nKO mice. In addition, the recovery of autophagy in *seipin*-nKO mice treated with PI3K or mTOR inhibitor reduced the levels of oligomeric tau protein or the tau phosphorylation, but did not alter the level of monomeric tau. A possible reason might be that the mTOR inhibition reduces the aggregation of tau protein via pathways other than autophagy (King et al., 2008). Thus, further studies are needed to elucidate this problem.

The hyperphosphorylated tau at Ser^{396} and insulin resistance appeared synchronously in *seipin*-sKO mice. An increase in tau phosphorylation at Ser^{396} residue is reported in streptozotocin (STZ)-induced type 1 diabetes rats (Santos et al., 2014). Consistent with clinical results in diabetic AD patients, the administration of rosi can relieve brain tau phosphorylation in type 2 diabetes rat models (Yoon et al., 2010). Thet pioglitazone treatment in *seipin*-sKO mice improved insulin resistance (Prieur et al., 2013). The treatment with rosi in *seipin*-sKO mice for 30 days corrected the hyperphosphorylated tau at Ser^{396}. Thus, it is highly likely that the insulin resistance in *seipin*-sKO mice is responsible for hyperphosphorylation of tau at Ser^{396}. The insulin signaling was impaired in the liver and adipose tissue of *seipin*-sKO mice (Cui et al., 2011). The impairment of insulin signaling may result in an inefficient activation of Akt-GSK3β signaling that leads to an enhanced tau phosphorylation (Tokutake et al., 2012). Clodfelder-Miller et al. (2006) reported that STZ diabetic animals present an increase in p38 MAPK and JNK active forms. The level of JNK phosphorylation in *seipin*-sKO mice was elevated. The JNK signaling is involved in insulin resistance and tau phosphorylation in AD transgenic mouse models (Ma et al., 2009). The effect of rosi on tau phosphorylation is attributable to JNK inactivation (Yoon et al., 2010). We observed that the treatment with rosi for 30 days corrected the level of JNK phosphorylation, but the GSK3β or mTOR inhibitor could not. In particular, the administration of the JNK inhibitor for 7 days in *seipin*-sKO mice was able to block the increase in tau phosphorylation at Ser^{396}, but not Thr^{212}/Ser^{214} and Ser^{202}/Thr^{205}. Thus, a possibility is that the insulin resistance in *seipin*-sKO mice through triggering JNK signaling induces tau phosphorylation at Ser^{396} (Fig. 7).

5. Conclusions

A large number of phosphorylation sites are detected on Alzheimer tau protein, suggesting that a single kinase is unlikely to activate all of these residues and hence multiple kinases might be involved. The neuronal seipin deletion causes the hyperphosphorylation tau at Thr^{212}/Ser^{214} and Ser^{202}/Thr^{205}, while seipin deletion-induced insulin resistance enhances the tau phosphorylation at Ser^{396}. The function of tau phosphorylation is related largely to stabilizing microtubules, whereas excessive or sustained tau phosphorylation impairs tau function. Indeed, the decrease and derangement of NF-H positive fibers and reduction of NF-H protein were observed in *seipin*-sKO mice and *seipin*-nKO mice, indicating axonal atrophy and degeneration. Although much more work needs to be performed in the future, this is the first report to demonstrate that seipin expression in hippocampal neurons is required for balancing tau phosphorylation to prevent neurodegeneration.

Competing interests

The authors declare that they have no competing interests.

Funding

This work was supported by National Natural Science Foundation of China (81471157; 81671253), Key Projects of Jiangsu Science and Technology Department of China (BE2016765), Jiangsu provincial Cadre health care research of China (BJ16014).

Authors' contributions

Huangxian Chang and Tingting Di managed the experimental protocol, directed all experiments and wrote draft of the manuscript. Ya Wang carried out the animal care. Guoxi Li aided in tissue preparation and data analysis. Ling Chen carried out the experimental design and the preparation of the manuscript. Qi Wang and Xianying Zeng edited the manuscript. All authors contributed to and have approved the final manuscript.

References

Agarwal, A.K., Garg, A., 2003. Congenital generalized lipodystrophy: significance of triglyceride biosynthetic pathways. Trends Endocrinol. Metab. 14, 214–221. https://doi.org/10.1016/S1043-2760(03)00078-X.

Caccamo, A., Majumder, S., Richardson, A., Strong, R., Oddo, S., 2010. Molecular interplay between mammalian target of rapamycin (mTOR), amyloid-beta, and tau: effects on cognitive impairments. J. Biol. Chem. 285, 13107–13120. https://doi.org/10.1074/jbc.M110.100420.

Caccamo, A., Magri, A., Medina, D.X., Wisely, E.V., Lopez-Aranda, M.F., Silva, A.J., Oddo, S., 2013. mTOR regulates tau phosphorylation and degradation: implications for Alzheimer's disease and other tauopathies. Aging Cell 12, 370–380. https://doi.org/10.1111/acel.12057.

Cai, W., Zhu, Y., Furuya, K., Li, Z., Sokabe, M., Chen, L., 2008. Two different molecular mechanisms underlying progesterone neuroprotection against ischemic brain damage. Neuropharmacology 55, 127–138. https://doi.org/10.1016/j.neuropharm.2008.04.023.

Cai, Z., Zhao, B., Li, K., Zhang, L., Li, C., Quazi, S.H., Tan, Y., 2012. Mammalian target of rapamycin: a valid therapeutic target through the autophagy pathway for Alzheimer's disease? J. Neurosci. Res. 90, 1105–1118. https://doi.org/10.1002/jnr.23011.

Camacho, I.E., Serneels, L., Spittaels, K., Merchiers, P., Dominguez, D., De Strooper, B., 2004. Peroxisome-proliferator-activated receptor gamma induces a clearance mechanism for the amyloid-beta peptide. J. Neurosci. 24, 10908–10917. https://doi.org/10.1523/JNEUROSCI.3987-04.2004.

Chen, W., Chang, B., Saha, P., Hartig, S.M., Li, L., Reddy, V.T., Yang, Y., Yechoor, V., Mancini, M.A., Chan, L., 2012. Berardinelli-seip congenital lipodystrophy 2/seipin is a cell-autonomous regulator of lipolysis essential for adipocyte differentiation. Mol. Cell. Biol. 32, 1099–1111. https://doi.org/10.1128/MCB.06465-11.

Clodfelder-Miller, B.J., Zmijewska, A.A., Johnson, G.V., Jope, R.S., 2006. Tau is hyperphosphorylated at multiple sites in mouse brain in vivo after streptozotocin-induced insulin deficiency. Diabetes 55, 3320–3325. https://doi.org/10.2337/db06-0485.

Cui, X., Wang, Y., Tang, Y., Liu, Y., Zhao, L., Deng, J., Xu, G., Peng, X., Ju, S., Liu, G., Yang, H., 2011. Seipin ablation in mice results in severe generalized lipodystrophy. Hum. Mol. Genet. 20, 3022–3030. https://doi.org/10.1093/hmg/ddr205.

Denner, L.A., Rodriguez-Rivera, J., Haidacher, S.J., Jahrling, J.B., Carmical, J.R., Hernandez, C.M., Zhao, Y., Sadygov, R.G., Starkey, J.M., Spratt, H., Luxon, B.A., Wood, T.G., Dineley, K.T., 2012. Cognitive enhancement with rosiglitazone links the hippocampal PPARgamma and ERK MAPK signaling pathways. J. Neurosci. 32, 16725–16735a. https://doi.org/10.1523/JNEUROSCI.2153-12.2012.

Ebihara, C., Ebihara, K., Aizawa-Abe, M., Mashimo, T., Tomita, T., Zhao, M., Gumbilai, V., Kusakabe, T., Yamamoto, Y., Aotani, D., Yamamoto-Kataoka, S., Sakai, T., Hosoda, K., Serikawa, T., Nakao, K., 2015. Seipin is necessary for normal brain

development and spermatogenesis in addition to adipogenesis. Hum. Mol. Genet. 24, 4238–4249. https://doi.org/10.1093/hmg/ddv156.
Escribano, L., Simon, A.M., Gimeno, E., Cuadrado-Tejedor, M., Lopez de Maturana, R., Garcia-Osta, A., Ricobaraza, A., Perez-Mediavilla, A., Del Rio, J., Frechilla, D., 2010. Rosiglitazone rescues memory impairment in Alzheimer's transgenic mice: mechanisms involving a reduced amyloid and tau pathology. Neuropsychopharmacology 35, 1593–1604. https://doi.org/10.1038/npp.2010.32.
Gendron, T.F., Petrucelli, L., 2009. The role of tau in neurodegeneration. Mol. Neurodegener. 4, 13. https://doi.org/10.1186/1750-1326-4-13.
Harrington, L.S., Findlay, G.M., Lamb, R.F., 2005. Restraining PI3K: mTOR signalling goes back to the membrane. Trends Biochem. Sci. 30, 35–42. https://doi.org/10.1016/j.tibs.2004.11.003.
Hu, J., Ramshesh, V.K., McGill, M.R., Jaeschke, H., Lemasters, J.J., 2016. Low dose acetaminophen induces reversible mitochondrial dysfunction associated with transient c-Jun N-terminal kinase activation in mouse liver. Toxicol. Sci. 150, 204–215. https://doi.org/10.1093/toxsci/kfv319.
Hua, X., Cao, X.Y., Wang, X.L., Sun, P., Chen, L., 2017. Exposure of pregnant mice to Triclosan causes insulin resistance via Thyroxine reduction. Toxicol. Sci. 160, 150–160. https://doi.org/10.1093/toxsci/kfx166.
Inestrosa, N.C., Godoy, J.A., Quintanilla, R.A., Koenig, C.S., Bronfman, M., 2005. Peroxisome proliferator-activated receptor gamma is expressed in hippocampal neurons and its activation prevents beta-amyloid neurodegeneration: role of Wnt signaling. Exp. Cell Res. 304, 91–104. https://doi.org/10.1016/j.yexcr.2004.09.032.
Ishizawa, T., Sahara, N., Ishiguro, K., Kersh, J., McGowan, E., Lewis, J., Hutton, M., Dickson, D.W., Yen, S.H., 2003. Co-localization of glycogen synthase kinase-3 with neurofibrillary tangles and granulovacuolar degeneration in transgenic mice. Am. J. Pathol. 163, 1057–1067. https://doi.org/10.1016/s0002-9440(10)63465-7.
Janson, J., Laedtke, T., Parisi, J.E., O'Brien, P., Petersen, R.C., Butler, P.C., 2004. Increased risk of type 2 diabetes in Alzheimer disease. Diabetes 53, 474–481. https://doi.org/10.1111/j.1582-4934.2011.01384.x.
Ji, C., Tang, M., Zeidler, C., Hohfeld, J., Johnson, G.V., 2019. BAG3 and SYNPO (synaptopodin) facilitate phospho-MAPT/tau degradation via autophagy in neuronal processes. Autophagy. https://doi.org/10.1080/15548627.2019.1580096.
Kilkenny, C., Browne, W.J., Cuthill, I.C., Emerson, M., Altman, D.G., 2012. Improving bioscience research reporting: the ARRIVE guidelines for reporting animal research. Osteoarthr. Cartil. 20, 256–260. https://doi.org/10.1016/j.joca.2012.02.010.
King, M.A., Hands, S., Hafiz, F., Mizushima, N., Tolkovsky, A.M., Wyttenbach, A., 2008. Rapamycin inhibits polyglutamine aggregation independently of autophagy by reducing protein synthesis. Mol. Pharmacol. 73, 1052–1063. https://doi.org/10.1124/mol.107.043398.
Kodl, C.T., Seaquist, E.R., 2008. Cognitive dysfunction and diabetes mellitus. Endocr. Rev. 29, 494–511. https://doi.org/10.1210/er.2007-0034.
Kruger, U., Wang, Y., Kumar, S., Mandelkow, E.M., 2012. Autophagic degradation of tau in primary neurons and its enhancement by trehalose. Neurobiol. Aging 33, 2291–2305. https://doi.org/10.1016/j.neurobiolaging.2011.11.009.
Levine, B., Kroemer, G., 2008. Autophagy in the pathogenesis of disease. Cell 132, 27–42. https://doi.org/10.1016/j.cell.2007.12.018.
Leyk, J., Goldbaum, O., Noack, M., Richter-Landsberg, C., 2015. Inhibition of HDAC6 modifies tau inclusion body formation and impairs autophagic clearance. J. Mol. Neurosci. 55, 1031–1046. https://doi.org/10.1007/s12031-014-0460-y.
Li, L., Xu, B., Zhu, Y., Chen, L., Sokabe, M., Chen, L., 2010. DHEA prevents Abeta25-35-impaired survival of newborn neurons in the dentate gyrus through a modulation of PI3K-Akt-mTOR signaling. Neuropharmacology 59, 323–333. https://doi.org/10.1016/j.neuropharm.2010.02.009.
Li, G., Zhou, L., Zhu, Y., Wang, C., Sha, S., Xian, X., Ji, Y., Liu, G., Chen, L., 2015. Seipin knockout in mice impairs stem cell proliferation and progenitor cell differentiation in the adult hippocampal dentate gyrus via reduced levels of PPARgamma. Dis. Model. Mech. 8, 1615–1624. https://doi.org/10.1242/dmm.021550.
Liu, Y., Su, Y., Wang, J., Sun, S., Wang, T., Qiao, X., Run, X., Li, H., Liang, Z., 2013. Rapamycin decreases tau phosphorylation at Ser214 through regulation of cAMP-dependent kinase. Neurochem. Int. 62, 458–467. https://doi.org/10.1016/j.neuint.2013.01.014.
Liu, L., Jiang, Q., Wang, X., Zhang, Y., Lin, R.C., Lam, S.M., Shui, G., Zhou, L., Li, P., Wang, Y., Cui, X., Gao, M., Zhang, L., Lv, Y., Xu, G., Liu, G., Zhao, D., Yang, H., 2014. Adipose-specific knockout of SEIPIN/BSCL2 results in progressive lipodystrophy. Diabetes 63, 2320–2331. https://doi.org/10.2337/db13-0729.
Ma, Q.L., Yang, F., Rosario, E.R., Ubeda, O.J., Beech, W., Gant, D.J., Chen, P.P., Hudspeth, B., Chen, C., Zhao, Y., Vinters, H.V., Frautschy, S.A., Cole, G.M., 2009. Beta-amyloid oligomers induce phosphorylation of tau and inactivation of insulin receptor substrate via c-Jun N-terminal kinase signaling: suppression by omega-3 fatty acids and curcumin. J. Neurosci. 29, 9078–9089. https://doi.org/10.1523/JNEUROSCI.1071-09.2009.
Magre, J., Delepine, M., Khallouf, E., Gedde-Dahl Jr., T., Van Maldergem, L., Sobel, E., Papp, J., Meier, M., Megarbane, A., Bachy, A., Verloes, A., d'Abronzo, F.H., Seemanova, E., Assan, R., Baudic, N., Bourut, C., Czernichow, P., Huet, F., Grigorescu, F., de Kerdanet, M., Lacombe, D., Labrune, P., Lanza, M., Loret, H., Matsuda, F., Navarro, J., Nivelon-Chevalier, A., Polak, M., Robert, J.J., Tric, P., Tubiana-Rufi, N., Vigouroux, C., Weissenbach, J., Savasta, S., Maassen, J.A., Trygstad, O., Bogalho, P., Freitas, P., Medina, J.L., Bonnicci, F., Joffe, B.I., Loyson, G., Panz, V.R., Raal, F.J., O'Rahilly, S., Stephenson, T., Kahn, C.R., Lathrop, M., Capeau, J., 2001. Identification of the gene altered in Berardinelli-Seip congenital lipodystrophy on chromosome 11q13. Nat. Genet. 28, 365–370. https://doi.org/10.1038/ng585.
Martinez, A., Alonso, M., Castro, A., Perez, C., Moreno, F.J., 2002. First non-ATP competitive glycogen synthase kinase 3 beta (GSK-3beta) inhibitors: thiadiazolidinones (TDZD) as potential drugs for the treatment of Alzheimer's disease. J. Med. Chem. 45, 1292–1299. https://doi.org/10.1021/jm011020u.
Martins, D.F., Rosa, A.O., Gadotti, V.M., Mazzardo-Martins, L., Nascimento, F.P., Egea, J., Lopez, M.G., Santos, A.R., 2011. The antinociceptive effects of AR-A014418, a selective inhibitor of glycogen synthase kinase-3 beta, in mice. J. Pain 12, 315–322.
Mizushima, N., Levine, B., Cuervo, A.M., Klionsky, D.J., 2008. Autophagy fights disease through cellular self-digestion. Nature 451, 1069–1075. https://doi.org/10.1016/j.jpain.2010.06.007.
Mocanu, M.M., Nissen, A., Eckermann, K., Khlistunova, I., Biernat, J., Drexler, D., Petrova, O., Schonig, K., Bujard, H., Mandelkow, E., Zhou, L., Rune, G., Mandelkow, E.M., 2008. The potential for beta-structure in the repeat domain of tau protein determines aggregation, synaptic decay, neuronal loss, and coassembly with endogenous Tau in inducible mouse models of tauopathy. J. Neurosci. 28, 737–748. https://doi.org/10.1523/JNEUROSCI.2824-07.2008.
Nishimura, I., Yang, Y., Lu, B., 2004. PAR-1 kinase plays an initiator role in a temporally ordered phosphorylation process that confers tau toxicity in *Drosophila*. Cell 116, 671–682. https://doi.org/10.1016/s0092-8674(04)00170-9.
Owen, B.M., Ding, X., Morgan, D.A., Coate, K.C., Bookout, A.L., Rahmouni, K., Kliewer, S.A., Mangelsdorf, D.J., 2014. FGF21 acts centrally to induce sympathetic nerve activity, energy expenditure, and weight loss. Cell Metab. 20, 670–677. https://doi.org/10.1016/j.cmet.2014.07.012.
Planel, E., Tatebayashi, Y., Miyasaka, T., Liu, L., Wang, L., Herman, M., Yu, W.H., Luchsinger, J.A., Wadzinski, B., Duff, K.E., Takashima, A., 2007. Insulin dysfunction induces in vivo tau hyperphosphorylation through distinct mechanisms. J. Neurosci. 27, 13635–13648. https://doi.org/10.1523/jneurosci.3949-07.2007.
Plattner, F., Angelo, M., Giese, K.P., 2006. The roles of cyclin-dependent kinase 5 and glycogen synthase kinase 3 in tau hyperphosphorylation. J. Biol. Chem. 281, 25457–25465. https://doi.org/10.1074/jbc.M603469200.
Prieur, X., Dollet, L., Takahashi, M., Nemani, M., Pillot, B., Le May, C., Mounier, C., Takigawa-Imamura, H., Zelenika, D., Matsuda, F., Feve, B., Capeau, J., Lathrop, M., Costet, P., Cariou, B., Magre, J., 2013. Thiazolidinediones partially reverse the metabolic disturbances observed in Bscl2/seipin-deficient mice. Diabetologia 56, 1813–1825. https://doi.org/10.1007/s00125-013-2926-9.
Qian, Y., Yin, J., Hong, J., Li, G., Zhang, B., Liu, G., Wan, Q., Chen, L., 2016. Neuronal seipin knockout facilitates Abeta-induced neuroinflammation and neurotoxicity via reduction of PPARgamma in hippocampus of mouse. J. Neuroinflammation 13, 145. https://doi.org/10.1186/s12974-016-0598-3.
Rajab, A., Khaburi, M., Spranger, S., Kunze, J., Spranger, J., 2003. Congenital generalized lipodystrophy, mental retardation, deafness, short stature, and slender bones: a newly recognized syndrome? Am. J. Med. Genet. A 121a, 271–276. https://doi.org/10.1002/ajmg.a.20245.
Santos, R.X., Correia, S.C., Alves, M.G., Oliveira, P.F., Cardoso, S., Carvalho, C., Duarte, A.I., Santos, M.S., Moreira, P.I., 2014. Insulin therapy modulates mitochondrial dynamics and biogenesis, autophagy and tau protein phosphorylation in the brain of type 1 diabetic rats. Biochim. Biophys. Acta 1842, 1154–1166. https://doi.org/10.1016/j.bbadis.2014.04.011.
Schaeffer, V., Goedert, M., 2012. Stimulation of autophagy is neuroprotective in a mouse model of human tauopathy. Autophagy 8, 1686–1687. https://doi.org/10.4161/auto.21488.
Sun, H., Kim, J.K., Mortensen, R., Mutyaba, L.P., Hankenson, K.D., Krebsbach, P.H., 2013. Osteoblast-targeted suppression of PPARgamma increases osteogenesis through activation of mTOR signaling. Stem Cells 31, 2183–2192. https://doi.org/10.1002/stem.1455.
Tokutake, T., Kasuga, K., Yajima, R., Sekine, Y., Tezuka, T., Nishizawa, M., Ikeuchi, T., 2012. Hyperphosphorylation of tau induced by naturally secreted amyloid-beta at nanomolar concentrations is modulated by insulin-dependent Akt-GSK3beta signaling pathway. J. Biol. Chem. 287, 35222–35233. https://doi.org/10.1074/jbc.M112.348300.
Van Maldergem, L., Magre, J., Khallouf, T.E., Gedde-Dahl Jr., T., Delepine, M., Trygstad, O., Seemanova, E., Stephenson, T., Albott, C.S., Bonnici, F., Panz, V.R., Medina, J.L., Bogalho, P., Huet, F., Savasta, S., Verloes, A., Robert, J.J., Loret, H., De Kerdanet, M., Tubiana-Rufi, N., Megarbane, A., Maassen, J., Polak, M., Lacombe, D., Kahn, C.R., Silveira, E.L., D'Abronzo, F.H., Grigorescu, F., Lathrop, M., Capeau, J., O'Rahilly, S., 2002. Genotype-phenotype relationships in Berardinelli-Seip congenital lipodystrophy. J. Med. Genet. 39, 722–733. https://doi.org/10.1136/jmg.39.10.722.
Vasheghani, F., Zhang, Y., Li, Y.H., Blati, M., Fahmi, H., Lussier, B., Roughley, P., Lagares, D., Endisha, H., Saffar, B., Lajeunesse, D., Marshall, W.K., Rampersaud, Y.R., Mahomed, N.N., Gandhi, R., Pelletier, J.P., Martel-Pelletier, J., Kapoor, M., 2015. PPARgamma deficiency results in severe, accelerated osteoarthritis associated with aberrant mTOR signalling in the articular cartilage. Ann. Rheum. Dis. 74, 569–578. https://doi.org/10.1136/annrheumdis-2014-205743.
Wang, J.Z., Gao, X., Wang, Z.H., 2014. The physiology and pathology of microtubule-associated protein tau. Essays Biochem. 56, 111–123. https://doi.org/10.1042/bse0560111.
Wang, L., Hong, J., Wu, Y., Liu, G., Yu, W., Chen, L., 2018. Seipin deficiency in mice causes loss of dopaminergic neurons via aggregation and phosphorylation of alpha-synuclein and neuroinflammation. Cell Death Dis. 9, 440. https://doi.org/10.1038/s41419-018-0471-7.
Watari, H., Shimada, Y., 2014. New treatment for Alzheimer's disease, Kamikihito, reverses amyloid-beta-induced progression of tau phosphorylation and axonal atrophy. Evid. Based Complement. Alternat. Med. 2014, 706487. https://doi.org/10.1155/2014/706487.
Wring, S., Murphy, G., Atiee, G., Corr, C., Hyman, M., Willett, M., Angulo, D., 2018. Lack of impact by SCY-078, a first-in-class Oral fungicidal Glucan synthase inhibitor, on the pharmacokinetics of rosiglitazone, a substrate for CYP450 2C8, supports the low risk for clinically relevant metabolic drug-drug interactions. J. Clin. Pharmacol. 58, 1305–1313. https://doi.org/10.1002/jcph.1146.

Yoon, S.Y., Park, J.S., Choi, J.E., Choi, J.M., Lee, W.J., Kim, S.W., Kim, D.H., 2010. Rosiglitazone reduces tau phosphorylation via JNK inhibition in the hippocampus of rats with type 2 diabetes and tau transfected SH-SY5Y cells. Neurobiol. Dis. 40, 449–455. https://doi.org/10.1016/j.nbd.2010.07.005.

Zhang, Y., Vasheghani, F., Li, Y.H., Blati, M., Simeone, K., Fahmi, H., Lussier, B., Roughley, P., Lagares, D., Pelletier, J.P., Martel-Pelletier, J., Kapoor, M., 2015. Cartilage-specific deletion of mTOR upregulates autophagy and protects mice from osteoarthritis. Ann. Rheum. Dis. 74, 1432–1440. https://doi.org/10.1016/j.joca.2014.02.631.

Zhang, Z.H., Wu, Q.Y., Zheng, R., Chen, C., Chen, Y., Liu, Q., 2017. Selenomethionine mitigates cognitive decline by targeting both tau hyperphosphorylation and autophagic clearance in an Alzheimer's disease mouse model. J. Neurosci. 37, 2449–2462. https://doi.org/10.1523/JNEUROSCI.3229-16.2017.

Zhang, Y., Huang, N.Q., Yan, F., Jin, H., Zhou, S.Y., Shi, J.S., Jin, F., 2018. Diabetes mellitus and Alzheimer's disease: GSK-3beta as a potential link. Behav. Brain Res. 339, 57–65. https://doi.org/10.1016/j.bbr.2017.11.015.

Zhou, J., Zhang, W., Liang, B., Casimiro, M.C., Whitaker-Menezes, D., Wang, M., Lisanti, M.P., Lanza-Jacoby, S., Pestell, R.G., Wang, C., 2009. PPARgamma activation induces autophagy in breast cancer cells. Int. J. Biochem. Cell Biol. 41, 2334–2342. https://doi.org/10.1016/j.biocel.2009.06.007.

Zhou, L., Yin, J., Wang, C., Liao, J., Liu, G., Chen, L., 2014. Lack of seipin in neurons results in anxiety- and depression-like behaviors via down regulation of PPARgamma. Hum. Mol. Genet. 23, 4094–4102. https://doi.org/10.1093/hmg/ddu126.

Zhou, L., Chen, T., Li, G., Wu, C., Wang, C., Li, L., Sha, S., Chen, L., Liu, G., Chen, L., 2016. Activation of PPARgamma ameliorates spatial cognitive deficits through restoring expression of AMPA receptors in Seipin Knock-out mice. J. Neurosci. 36, 1242–1253. https://doi.org/10.1523/JNEUROSCI.3280-15.2016.